Asian Journal of Scientific Research

ISSN 1992-1454

science alert
http://www.scialert.net

ANSInet
an open access publisher
http://ansinet.com

OPEN ACCESS Asian Journal of Scientific Research

ISSN 1992-1454
DOI: 10.3923/ajsr.2018.203.221

Research Article
New Technique for Elimination of Ferroresonant Oscillations in Series Capacitor of Power System

Seyyed Hamid Fathi and Ataollah Abbasi

Department of Electrical Engineering Faculty, Amirkabir University of Technology, 15875-4413 Tehran, Iran

Abstract

Background and Objective: The complex ferroresonant behavior in power transformers can create overvoltages and overcurrents resulting in damage to power system equipment and customer installations. It can also cause subharmonics and nonlinear harmonics in power system. In this study, a new method was proposed to control and damp ferroresonant oscillations, which is based on a new ferroresonance limiter (FL). **Materials and Methods:** In order to control ferroresonance oscillations, a saturating choke and damping resistor was used to eliminate all the unwanted ferroresonant states. Since the ferroresonance phenomenon in transformer was described by nonlinear dynamics, chaos theory was used to study this phenomenon. By using this theory, the changes in system parameters which can cause chaotic ferroresonant oscillations, can be reviewed and analyzed in detail. **Results:** The behavior of the system during ferroresonance occurrence, with and without using proposed ferroresonance limiter, are discussed in bifurcation and phase plane diagrams. By using these diagrams, the behavioral changes of the system can be easily seen in two cases. **Conclusion:** The simulation results strongly show the effectiveness of using the proposed FL for limiting ferroresonant oscillations and creating stable orbit in power transformer terminals that energized by series capacitors or transmission lines compensated.

Key words: Series capacitor, saturable choke, damping resistor, ferroresonant oscillations, power transformer

Received: August 13, 2017 Accepted: September 23, 2017 Published: March 15, 2018

Citation: Seyyed Hamid Fathi and Ataollah Abbasi, 2018. New technique for elimination of ferroresonant oscillations in series capacitor of power system. Asian J. Sci. Res., 11: 203-221.

Corresponding Author: Seyyed Hamid Fathi, Department of Electrical Engineering Faculty, Amirkabir University of Technology, 15875-4413 Tehran, Iran
Tel: +982164543353

Competing Interest: The authors have declared that no competing interest exists.

Data Availability: All relevant data are within the paper and its supporting information files.

INTRODUCTION

Ferroresonance is an electrical complex nonlinear phenomenon, which can create thermal and insulation failures in transmission and distribution systems. It may be initiated by contingency switching operation, lightning, routine switching, no load conditions, series compensation, load shedding or capacitor banks connection to the secondary of the transformer winding involving a high voltage transmission and distribution lines[1-5].

This phenomenon consists of multiple modes with different frequencies such as: Fundamental frequency, sub harmonic, quasi-periodic and chaotic modes[6-8]. The sudden transition or jump from one steady state to another is triggered by a disturbance, switching action or a gradual changes in values of a parameter. The ferroresonance causes overvoltage and over currents in power networks which not only can damage transformers but also may cause severe damages to network devices like series capacitors [9-14], Unlike the resonance, which occurs in RLC circuits with linear capacitances and inductances for a particular frequency, the ferroresonance is occurred in a circuit with a nonlinear inductance due to the core behavior of the transformer. The magnetic core of the transformer can be considered as a nonlinear inductance and composition of line to line, line to earth capacitances, series capacitors and grading capacitors of circuit breakers can be considered as a linear capacitance[15,16].

The ferroresonant oscillations are dependent of not only frequency but also other factors, such as system voltage magnitude, initial magnetic flux condition of transformer iron core, total core losses in the circuit and the switching moment[17,18].

The nonlinear nature of ferroresonance leads to these systems are considered to be nonlinear dynamic systems and linear methods cannot be used to analyze them. Analytical approaches based on graphical solutions have been proposed to show bifurcations in single-phase ferroresonance circuits[19,20]. In the ferroresonance, because of nonlinear characteristics of circuit elements, the number of fixed points is more than one. Thus by variation of system parameters, the fixed points lose their stability.

The bifurcation theory is a useful method for identifying system parameters lead to ferroresonance[21,22]. It enables us to describe and analyze qualitative properties of the solutions, i.e., the fixed points, when system parameters change. The researches based on bifurcation theory need relatively high computational burden and are only valid for limited cases. Some of these methods are valid only in limited cases while creating a bifurcation. However by using a continuation method, they can be more systematic and save computational muss[23-26].

There are several methods to limit and damp ferroresonant oscillations, such as using a suitable RLC filter, using damping reactors, using metal oxide arrester and neutral point resistance application in transformers. One of the problems of arresters is that during ferroresonant oscillations in distribution systems, they may burst[27-32].

In this study, for analyzing the ferroresonance, a nonlinear model of core losses is considered. Neve is given an algorithm for calculating core losses from no-load characteristics[33]. Bifurcation diagrams, phase plans, Feigenbaum numbers and Lyapunov exponents for analyzing route to chaos in ferroresonant behavior of the voltage transformer are used[34-36].

In order to obtain the eigen values, the method used is the multiple scales method[37]. Stability analysis by Lyapunov exponents and bifurcation diagrams is applied.

In this study, a saturating choke and damping resistor is used to control ferroresonance, transient and through fault currents. A small scale nonlinear single phase ferroresonant circuit was modeled with realistic/unit component values.

MATERIALS AND METHODS

Ferroresonance circuit and modeling: The three-phase diagram of the circuit studied by Al-Anbarri[38] is shown in Fig. 1.

The ferroresonance occurs in phase A, when this phase is switched off on the low-voltage side of the transformer, phase C is not connected to the transformer at that time. The transformer is modeled by a T-equivalent circuit with all impedances referred to the high voltage side. The magnetization branch is modeled by a nonlinear inductance in parallel with a nonlinear resistance, which represented by nonlinear saturation characteristic (λ-i_{Lm}) and nonlinear hysteresis and eddy current characteristics (v_m-i_{Rm}), respectively. The hysteresis and eddy current characteristics are calculated using the no-load characteristics and applying the algorithm given by Davarpanah[33]. The iron core saturation characteristic is given by the following equation:

$$i_{Lm} = a\lambda+b\lambda^{q} \quad (1)$$

where, λ is eigen value, a and b: Coefficient for magnetizing wave.

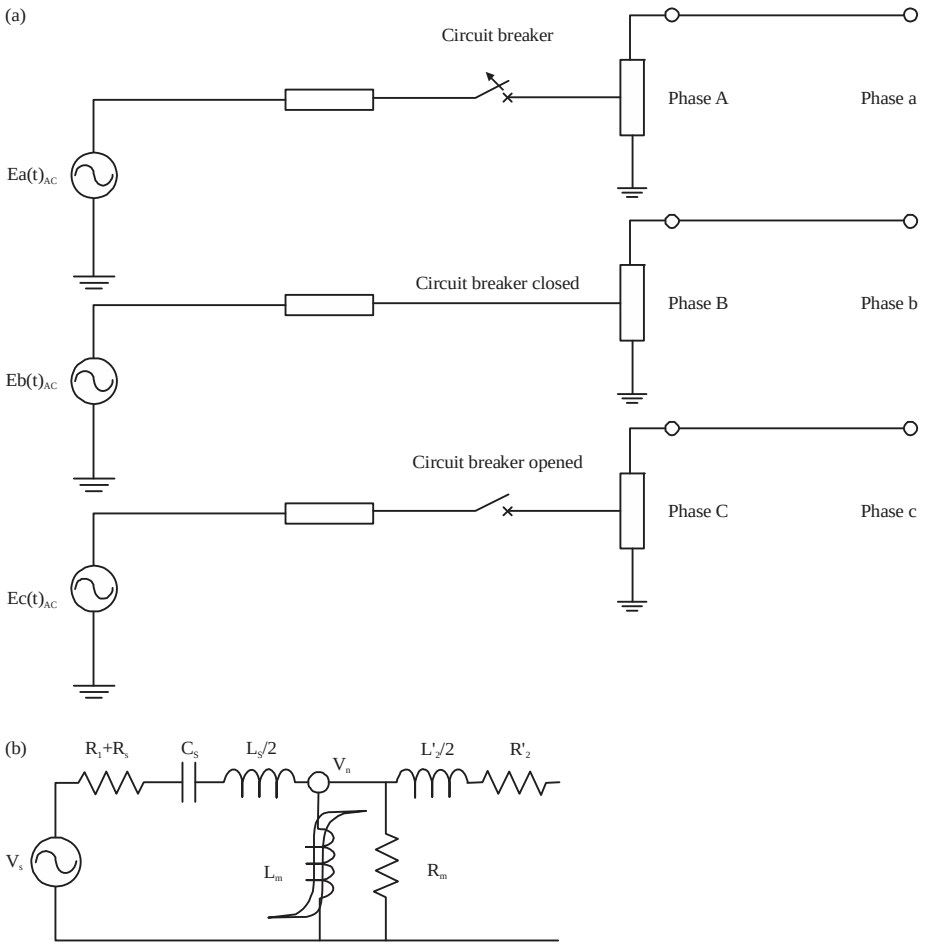

Fig. 1(a-b): (a) Ferroresonance circuit in no load transformer and b) T-equivalent circuit

The dynamics of the equivalent circuit can be described by the following nonlinear differential equation:

$$\frac{d^2\lambda}{dt^2}+\frac{1}{R(C_{sh}+C_{ser})}\frac{d\lambda}{dt}+\frac{1}{(C_{sh}+C_{ser})}(a\lambda+b\lambda^q)=\frac{C_{ser}\omega}{(C_{sh}+C_{ser})}\left(\sqrt{2}V_{rms}Cos\theta\right) \quad (2)$$

where, C_{ser} is series linear capacitor, C_{sh} is shunt linear capacitor.

The exponent q depends on the degree of saturation. For three different values of q, Coefficients a and b are selected as follows.

Prospective authors are:

for q = 11 a = 0.0067, b = 0.0001
for q = 7 a = 0.0067, b = 0.001
for q = 5 a = 0.0071, b = 0.0034

Using reference of Fig. 2, for q = 11, flux linkage curve via magnetization current in saturation section has less slope than what can be viewed for q = 5 and 7. Thus, ferroresonance effects appear earlier. Furthermore, increasing q will increase the number of stable and unstable points. Then changing in control parameters such as source voltage magnitude, may expose unstable points like saddle points and chaotic attractors as well.

The core losses are modeled with a switched resistor, which effectively reduced the core losses resistance by a factor of four at the time of the ferroresonance occurrence. In this study, the core losses model adopted is described by a third order power series whose coefficients are fitted to match the hysteresis and eddy current nonlinear characteristics as Eq. 3[38]:

$$i_{Rm}=-h_0+h_1v_m-h_2v_m^2+h_3v_m^3 \quad (3)$$

where, i_{Rm} is core loss current, v_m is terminal voltage of transformer and h_i are constant factors.

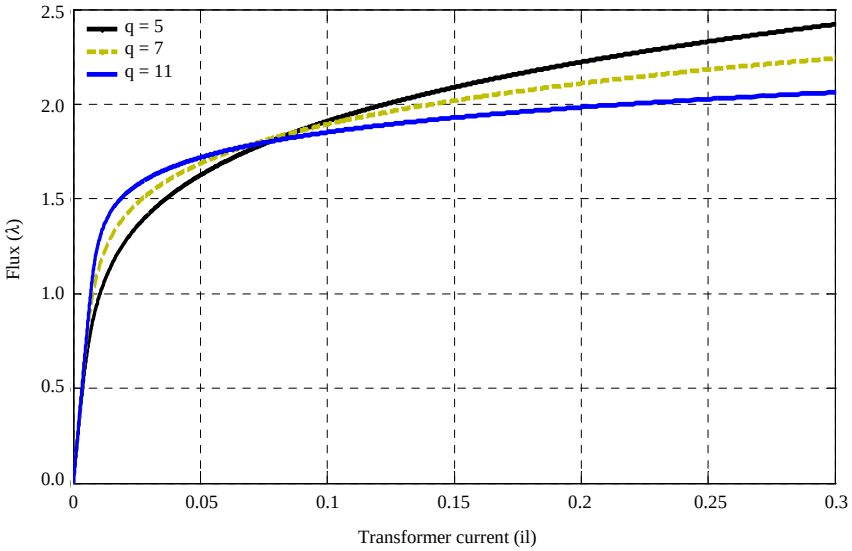

Fig. 2: Nonlinear saturation characteristic for three values of q

The per unit value of i_{Rm} for this case is determined by Eq. 4[32]:

$$i_{Rm} = -0.000001 + 0.0047\,v_m - 0.0073\,v_m^2 + 0.0039\,v_m^3 \quad (4)$$

The dynamic equation of the system is given by Eq. 5:

$$\frac{d^2\lambda}{dt^2} + \frac{1}{(C_{sh}+C_{ser})}\left(h_1\frac{d\lambda}{dt} + \left(h_2\frac{d\lambda}{dt}\right)^2 + \left(h_3\frac{d\lambda}{dt}\right)^3\right) + \frac{1}{(C_{sh}+C_{ser})}(a\lambda + b\lambda^q) + \frac{h_0}{(C_{sh}+C_{ser})} = \frac{C_{ser}}{(C_{sh}+C_{ser})}\left(\frac{d(E_s)}{dt}\right) \quad (5)$$

X_1, X_2, ε, μ and k are defined as the Eq. 6-10:

$$X_1 = \lambda \quad (6)$$

$$X_2 = V \quad (7)$$

$$\varepsilon = \frac{1}{(C_{sh}+C_{ser})} \quad (8)$$

$$\mu = \frac{1}{R} \quad (9)$$

$$K = C_{ser}\omega\left(\sqrt{2}V_{rms}\right) \quad (10)$$

By substituting parameters X_1, ε, μ and k in Eq. 5 and 11 will be obtain:

$$\ddot{X}_1 + \varepsilon\mu(aX_1 + bX_1^q) = K\varepsilon Cos\theta \quad (11)$$

State equations are given as Eq. 12 and 13:

$$\dot{X}_1 = X_2 \quad (12)$$

$$\dot{X}_2 = -\varepsilon\mu(aX_1 + bX_1^q) - \varepsilon\mu X_2 + K\varepsilon\varepsilon Cos\theta \quad (13)$$

If the state equations are considered as Eq. 14:

$$\dot{X} = AX + BU \quad (14)$$

where, matrixes X and U are state variables matrixes, system inputs and matrixes A and B represent matrix coefficients of state variables and system inputs, thus:

$$\dot{X} = \begin{bmatrix}\dot{X}_1\\ \dot{X}_2\end{bmatrix} = \begin{bmatrix}0 & 1\\ -a\varepsilon & -\varepsilon\mu\end{bmatrix}\begin{bmatrix}X_1\\ X_2\end{bmatrix} + \begin{bmatrix}0 & 0\\ -b\varepsilon & 0\end{bmatrix}\begin{bmatrix}X_1^q\\ 0\end{bmatrix} + \begin{bmatrix}0\\ K\varepsilon\end{bmatrix}U(t) \quad (15)$$

where, U(t) = Cos ωt. The fixed points or equilibrium points are defined the vanishing of the vector field, that is:

$$\dot{X} = 0 \quad (16)$$

At the fixed points, since the right-hand term of Eq. 14 becomes zero, stability is dominated by the eigen values of the jacobian, i.e.:

$$J = \frac{\partial f}{\partial x}$$

evaluated at the fixed points. The multiple scales method can be used as a simplification method for the stability and bifurcation analysis[37]. Using the multiple scales method, the first order approximation is obtained for the solution of Eq. 11 as:

$$X_1 = hCos(\omega t-\gamma)+O(\varepsilon) \quad (17)$$

The parameters μ, a and k are independent of ε. Furthermore, the frequency of system is as Eq. 18:

$$\omega = 1+\varepsilon\delta \quad (18)$$

where, δ is named the external detuning. By using the multiple scales method, the first order uniform expansion of Eq. 11 is obtained in the form:

$$X_1 (t, \varepsilon) = X_{1,0}(T_0, T_1)+\varepsilon X_{1,1}(T_0, T_1)+.... \quad (19)$$

where, $T_0 = t$ and $T1 = \varepsilon T_0$.

In the term of T_1 the time derivative becomes:

$$\frac{d}{dt} = D_0 + \varepsilon D_1 + \varepsilon^2 D_2 + ... \quad (20)$$

Substituting Eq. 19 and 20 into Eq. 11 and equating coefficient of power, ε, Eq. 21 and 22 are obtained:

$$\begin{aligned} &O(\varepsilon_0): \\ &D_0^2 X_{1,0} = 0 \end{aligned} \quad (21)$$

$$D_0^2 X_{1,1} + 2D_1 D_0 X_{1,0} + \mu D_0 X_{1,0} + bX_{1,1}^q = KCos\omega_0 t \quad (22)$$

The solution of Eq. 21 can be expressed as:

$$X_{1,0} = A(T_1)T_0+A_0 \quad (23)$$

Using multiple scales method the frequency response equations are yielded as Eq. 24:

$$a_0^2\delta^2 + \frac{1}{4}\alpha_0^2 = \frac{1}{4}K^2 \quad (24)$$

The stability of the fixed points depends on the eigen values of the jacobian matrix, that is, the eigen value of:

$$A = \begin{bmatrix} 1/2 & \frac{K}{2}Sin\beta \\ \frac{K}{2\alpha^2}Sin\beta & -\frac{K}{2}Cos\beta \end{bmatrix} \quad (25)$$

Determinant of $|\lambda I-A|$ yields eigen values:

$$\lambda^2 + (\frac{K}{2\alpha}Cos\beta)\lambda - \frac{K}{4\alpha}Cos\beta - \frac{K^2}{4\alpha^2}Sin^2\beta = 0 \quad (26)$$

where, λ is eigen value. By substituting the polar form of A into Eq. 20 and substituting result into Eq. 21, it will be found that the first approximation X_1 is given by Eq. 27:

$$X_1 = \alpha Cos(\omega t+\beta)+.... \quad (27)$$

$$\text{if} \quad K = 0 \xrightarrow{\text{yields}} \begin{cases} \alpha\beta = -\alpha\delta \\ \alpha' = -\frac{1}{2}\alpha \end{cases} \quad (28)$$

For nontrivial solutions, $\alpha \neq 0$ and it follows from Eq. 28 that:

$$\beta = -\delta T_1 + \beta_0, T_1 = \varepsilon t \xrightarrow{\text{yields}} \beta = -\varepsilon\delta t + \beta_0 \quad (29)$$

Substituting Eq. 29 into Eq. 27, it is found that to the first approximation, the free oscillations of Eq. 11 are given by Eq. 30:

$$X_1 = \alpha Cos(\omega_0 t+\beta_0)+\ldots \quad (30)$$

where, α is given by Eq. 28, which has the normal form of a supercritical pitchfork bifurcation. Eigen values can be obtained by Eq. 31:

$$\lambda^2 + \left(\frac{1}{2}\alpha_0 - \frac{1}{2}\right)\lambda - \frac{1}{4} - \delta^2 = 0 \quad (31)$$

RESULTS AND DISCUSSION

Circuit modeling without FL: The equivalent circuit of the ferroresonance circuit of Fig. 1 shown in Fig. 3.

This circuit can be modeled as shown in Fig. 4, where Z_{th} represents the Thevenin impedance.

In this section, initial value of circuit parameter is assumed in Table 1.

In this study subharmonic ferroresonance behavior in transformer without FL is studied. The results obtained by the two methods validate each other. The major analytical tools, used in this paper, to study subharmonic ferroresonance are phase plane and bifurcation diagrams.

The phase plane analysis is a graphical method, in which the time behaviour of a system is represented by the movement of state variables of the system in state space coordinates. As time elapses, the states position move on a trajectory. If the trajectory is a single closed line, then the system is periodic. In a chaotic system, however, the trajectory will never close on itself as the cycles are completed. A bifurcation diagram is a plot that displays single or multiple solutions (bifurcations) as the value of the control parameter is increased.

Table 1: Initial value of circuit parameters

V_{base}	L_S	C	R	R_{core}
11Kv	0.0188 p.u.	0.07955 p.u.	0.0014 p.u.	556.68 p.u.

V: Voltage, L_s: Series inductance R: Resistance, C: Current

Phase plane diagram and magnetization curve and voltage and flux waveforms are shown in Fig. 5-8 indicate the ferroresonant behaviour of the system at vin = 1.35 p.u. and q = 7. According to these Fig. 5-8, period doubling bifurcation has been occurred. These oscillations have an unwanted effect on system insulation and may harm it. The core current-flux linkage curve includes both eddy current and hysteresis losses.

The bifurcation diagram for q = 7 shown in Fig. 9, is the best diagram for exhibition of dynamic behavior of ferroresonance. Using this bifurcation diagram can analyze complexity of trajectories behavior in transformer. Blue route has main frequency of voltage source.

When V_{in} increases until V_{in} = 0.3125, voltage is stable. Frequency of output voltage is 50 Hz. Then at point (1) the voltage in terminal of transformer increases. The value of jumping voltage is 1.44. This voltage jump causes that the voltage amplitude reaches to 2.23 p.u. Fixed points remain stable and trajectories continue single frequency from path (A).

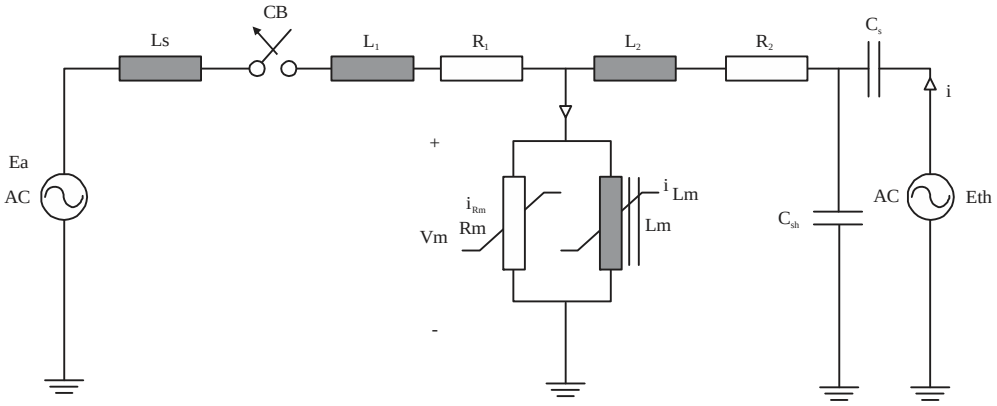

Fig. 3: Equivalent ferroresonance circuit

L_s: Series inductance, L_1: Leakage inductance, R_1: Leakage resistance, i_{Rm}: Loss current of magnetization branch, i_{Lm}: Magnetization current, [L_2, R_2, C_s, C_{sh}]: Load parameters, [E_a E_b]: Voltage source, Eth: Voltage thevenin

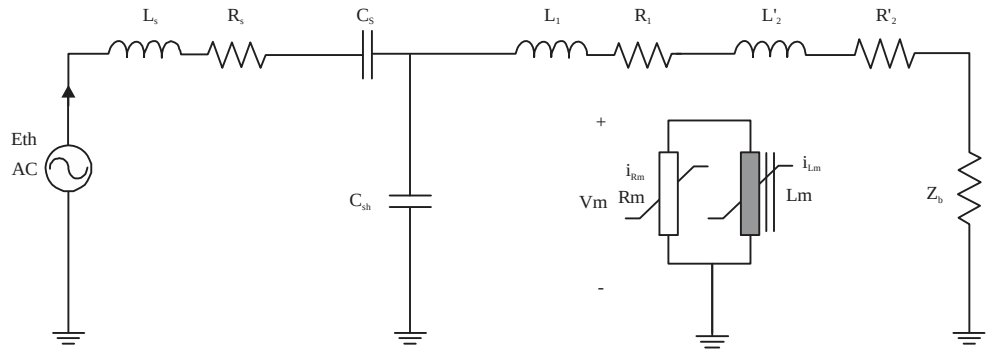

Fig. 4: Detailed model of ferroresonance circuit

L_s: Series inductance, L_1: Leakage inductance, R_1: Leakage resistance, i_{Rm}: Loss current of magnetization branch, i_{Lm}: Magnetization current, [L_2, R_2, C_s, C_{sh}]: Load parameters, [E_a E_b]: Voltage source, Eth: Voltage thevenin, Z_b: Impedance branch of load

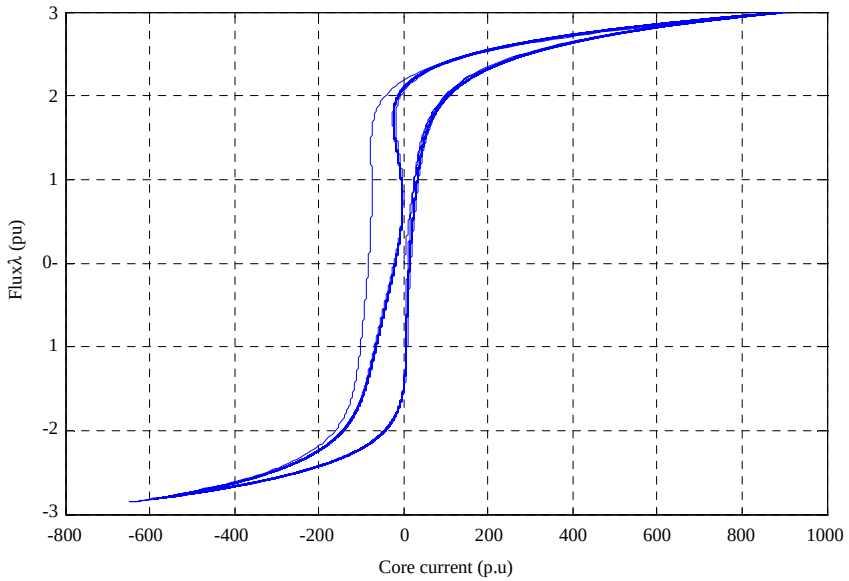

Fig. 5: Nonlinear transformer magnetization curve for nonlinear core losses model (V_{in} = 1.35 pu, q = 7)

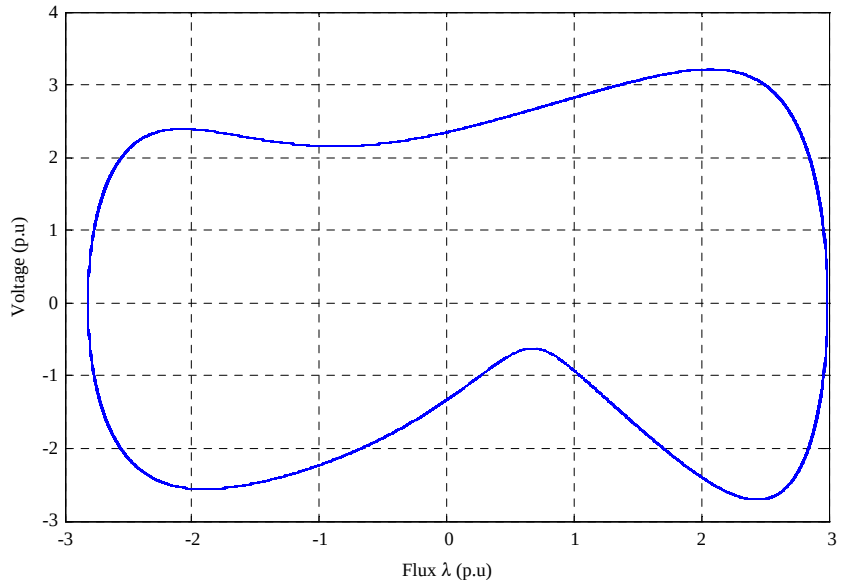

Fig. 6: Phase plane diagram of transformer for subharmonic ferroresonance mode at V_{in} = 1.35 pu, q = 7

At V_{in} = 0.5887 other path emerges in output voltage which continues from path (B) (green path). When V_{in} increases at V_{in} = 1.7325 other frequency emerges in output voltage (path C). At V_{in} = 2.992 p.u. at points (3-A), (3-B) and (3-C) in each path PDB(1) occurs. This behavior continues until at points (4-A), (4-B) and (4-C) in each path PDB(2) occurs. This process continues until system at points (5-A), (5-B) and (5-C) enters into chaotic regions. Border collision is shown in Fig. 9. In the Border collision system becomes chaotic suddenly.

Table 2: Eigen values for PDB

	Path		
PDB	A	B	C
PDB(1)	-2.32,-0.81	-3.19,-0.723	-1.84,-0.65
PDB(2)	-1.76,-0.46	-2.11,-0.134	-1.46,-0.31

Eigen values for PDB(1) and PDB(2) as shown in Table 2. The sequence of bifurcation parameters obeys a geometric law with a Feigenbaum constant[39]. This constant is gained as the following limit:

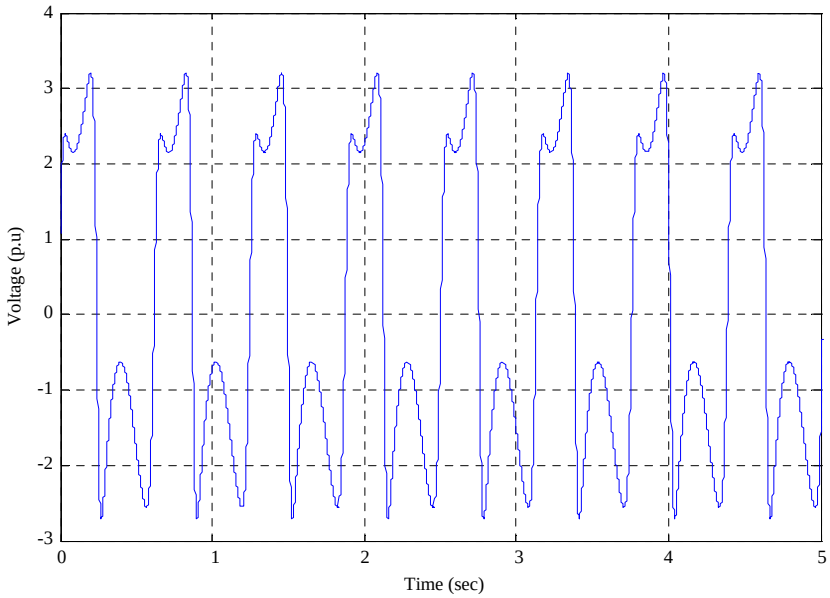

Fig. 7: Time-domain voltage waveform of transformer for subharmonic ferroresonance mode (V_{in} = 1.35 p.u., q = 7)

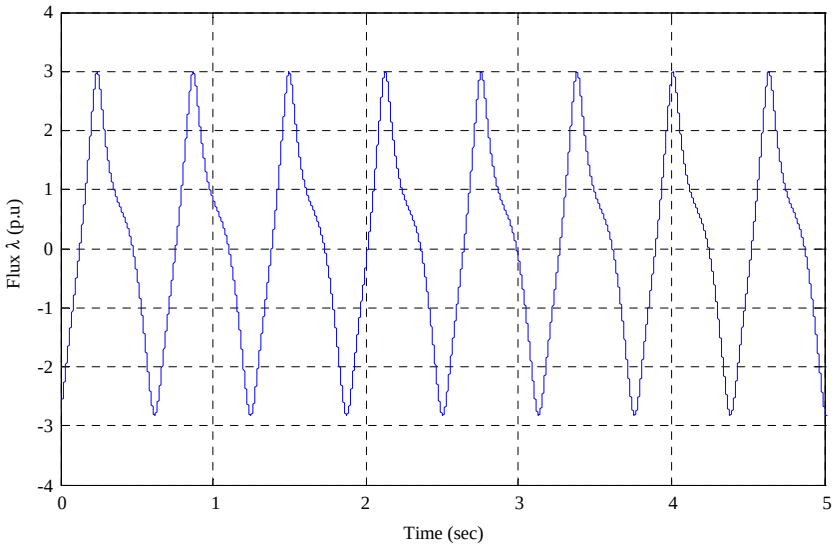

Fig. 8: Time-domain flux waveform of transformer for subharmonic ferroresonance mode (V_{in} = 1.35 p.u., q = 7)

$$\delta = \lim_{i\to\infty}\left\{\frac{a_i - a_{i-1}}{a_{i+1} - a_i}\right\} \approx 4.6692016 \quad (32)$$

$$\delta = \lim_{i\to\infty}\left\{\frac{8.001 - 1.7931}{9.3326 - 8.001}\right\} \approx 4.6694 \quad (33)$$

In practical applications the limit cannot be taken. An estimate of the Feigenbaum constant can be gained from a finite sequence.

In path (A):

- PDB(1): $a_{i-1} = a^1 = 1.7831$
- PDB(2): $a_i = a^2 = 8.001$
- PDB(3): $a_{i+1} = a^3 = 9.3326$

Delay in occurrence of chaos is because of damping section in core loss function. But it can be observed increasing q causes chaos occur in lower value of V_{in} than pervious bifurcation diagram. The nonlinear core loss model causes the mitigation in chaotic ferroresonance behavior in voltage transformer. Also presence of nonlinear term in core loss function in dynamic equations causes that period doubling logic in behavior of system becomes regular.

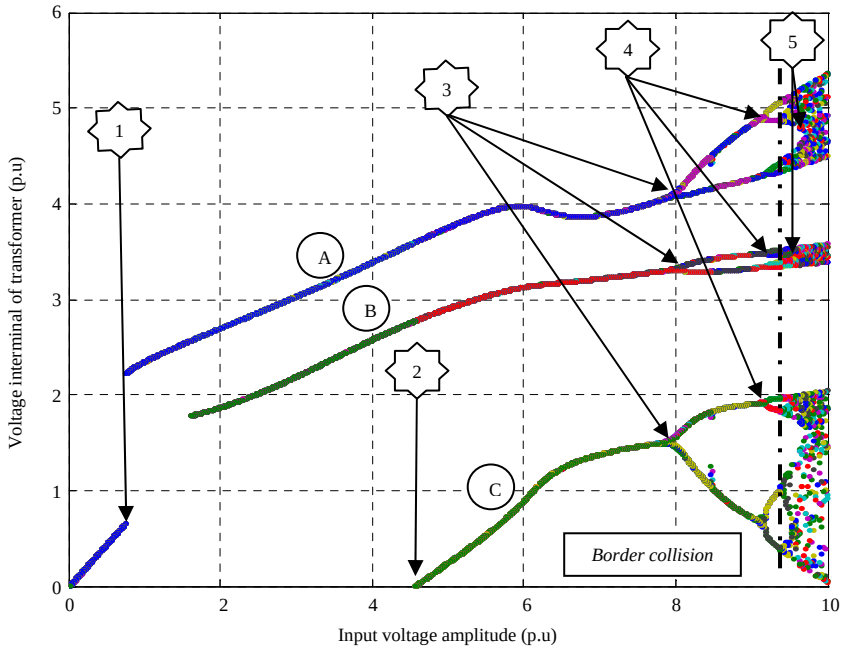

Fig. 9: Bifurcation diagram for nonlinear core loss model for q = 7 (bifurcation parameter: V_{in})
A, B and C are separate Chaotic Region, 1: Period one-two oscillations from A-B region, 2: Period one-two oscillations from B-C region, 3: Period one-two oscillations in A, B, C regions, 4: Period Two-four oscillations in A, B, C regions, 5: Border collision and rout to chaos

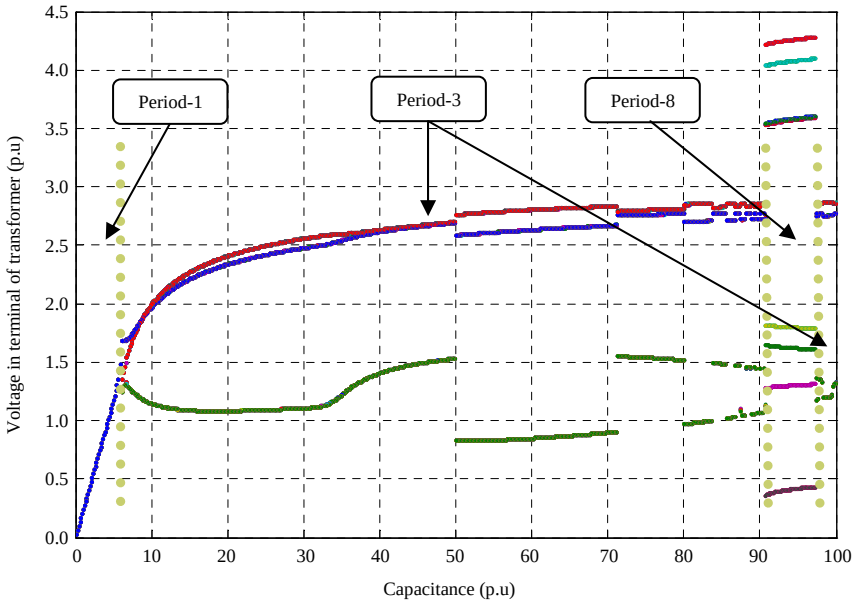

Fig. 10: Bifurcation diagram for nonlinear core loss model for q = 7 (bifurcation parameter: C_{sh})

Also bifurcation diagram is shown in Fig. 10 When the C_{sh} is selected as bifurcation parameter. This figure has been obtained for C_{sh} ranging from 0-100 p.u. under the same single-phase fault clearing condition. Figure 10 illustrates the existence of different types of bifurcation. For C_{sh} = 6 p.u., behavior of system is period-1 and fundamental mode and ferroresonance has not occurred. For C_{sh} 6-50 p.u., ferroresonant oscillations have three different frequencies

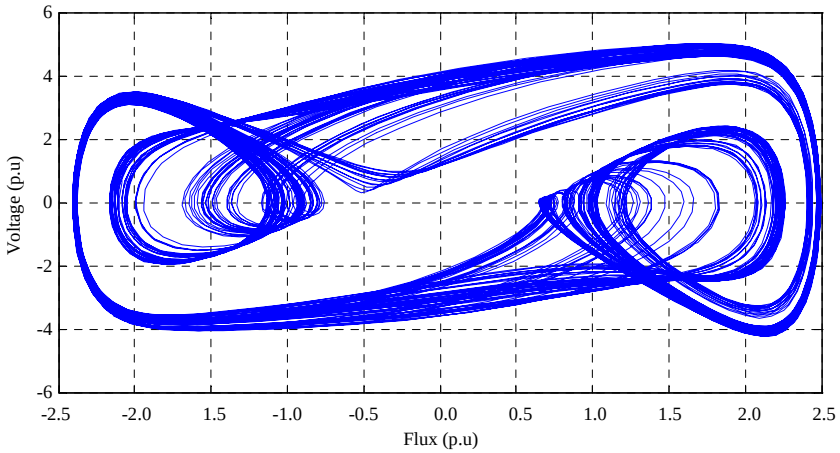

Fig. 11: Phase plane diagram of transformer for ferroresonance mode

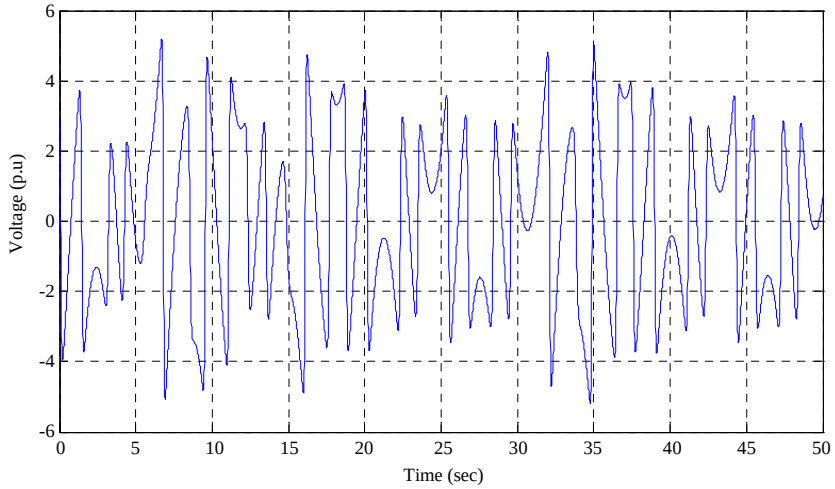

Fig. 12: Time-domain voltage waveform of transformer for ferroresonance mode

which are shown with blue (main frequency), green and red colour. For 50<C<80 pu. This behaviour continues and voltage jump occur. With increasing C_{shunt} 5-period and 6-period behaviour occurs, respectively and finally system becomes chaotic. As can be seen, this two bifurcation diagram is consistent with the two bifurcation diagram[40].

Phase plane diagram and voltage waveform of the system are shown in Fig. 11 and 12 for C_{shunt} = 189 p.u., V_{in} = 1 p.u, q = 7. As can be seen in these figures, for this C_{shunt}, chaotic ferroresonant oscillations in power system occurs.

Circuit modeling with FL (saturable choke and damping resistor): Modelling with series compensated circuits have shown what major problems ferrorcsonance and short circuit currents can be. The fundamental approach to overcoming these problems has often been to use protection devices to sense abnormal conditions of ferroresonance and short circuit and then bypass the capacitor with a switch or circuit breaker to protect the capacitor.

This approach requires expensive protection sensing equipment, switches/circuit breakers and other related equipment. During normal operation the circuit always remains susceptible to ferroresonance and heavy short circuit current. It is only when abnormal conditions are sensed by the protection that the circuit is altered to counteract the problems.

New techniques that can address the ferroresonance and short circuit issues with less protection equipment and reduced hardware requirements offer great potential benefits for the electricity supply industry.

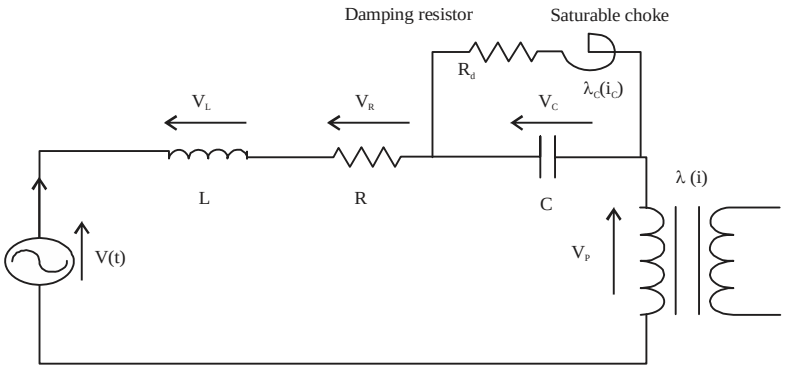

Fig. 13: Series compensated circuit with damping resistor and saturable choke

[1]λ(i): Transformer flux, λ_c(i): Choke flux, [L,R]: Source parameters, R_d : Damper resistor, V_p: Primary voltage, i: Current, V(t): Instantaneous value of the voltage, V_L: Instantaneous value of the inductance, V_R: Instantaneous value of the resistance, V_C: Instantaneous value of capacitor, C: Capacitor

A series compensated circuit configuration with a damping resistor and saturable choke is shown in Fig. 13. The transformer has a saturable iron core. The power line supplying the transformer is represented by a linear inductance "L" and resistance "R". The circuit contains a series capacitor to tune out the effects of the line inductance. The capacitance will normally be chosen so as to tune out all or most of the line inductance at the power frequency.

The use of a saturable choke in conjunction with the damping resistor is the innovative aspect of the circuit. Extensive modelling of this circuit shows that it has properties that are well suited to series compensation of distribution lines.

Theory of operation: The fundamental aspect of the series compensation circuit is that all circuit elements of the series compensator are permanently connected in the circuit. There are no switches or circuit breakers and no protection relays.

Under emergency full load conditions the voltage across the capacitor will typically reach 20% of the supply voltage. The saturating choke is designed such that at full emergency line loading, the knee point of the choke is sufficiently high so as not to interfere with the normal operation of the capacitor. Hence, under normal operating conditions the choke draws only a small magnetizing current and the capacitor effectively carries all the load current. This provides the line with the desired compensation effect.

Under conditions of subhannonic ferroresonance the capacitor voltage increases substantially above the knee point driving the choke into saturation. During saturation the choke looks like a short circuit which effectively places the damping resistor in parallel with the capacitor. Careful selection of components can eliminate the undesirable ferroresonant states. The low frequency components of the subhannonic ferroresonance also assists with saturating the choke.

Under fault short circuit conditions on the load side of the series compensator the capacitor voltage rises substantially above normal causing the choke to saturate. During the parts of the cycle where choke is saturated the damping resistors are effectively in parallel with the capacitor. This has the effect of reducing the overall line fault current and substantially reducing the fault current carried by the capacitor.

One of the significant circuit aspects of the saturable choke is that it provides a path for D.C. current to be bypassed around the capacitor. The location of the saturating choke ensures that the series capacitor holds no steady state D.C. component of voltage/charge. The circuit arrangement forces any D.C. component of capacitor charge to be discharged via the damping resistor and saturating choke. Trapped D.C. capacitor charge causes power transformer saturation which can lead to the onset of ferroresonance.

Circuit described earlier in this paper was used as the base circuit on which to model the series compensator technique. Figure 13 shows the series compensated circuit that was modeled with component values of below:

- L = 0.02 H, R = 1.55 Ω, C = 507 μF, R_d = 6.28, transformer: 11KV/400V rated at 3 MVA

The transformer was modelled with no load by Eq. 34 shown in Fig. 14:

$$i = 0.1\lambda+0.892\lambda^5 \quad (34)$$

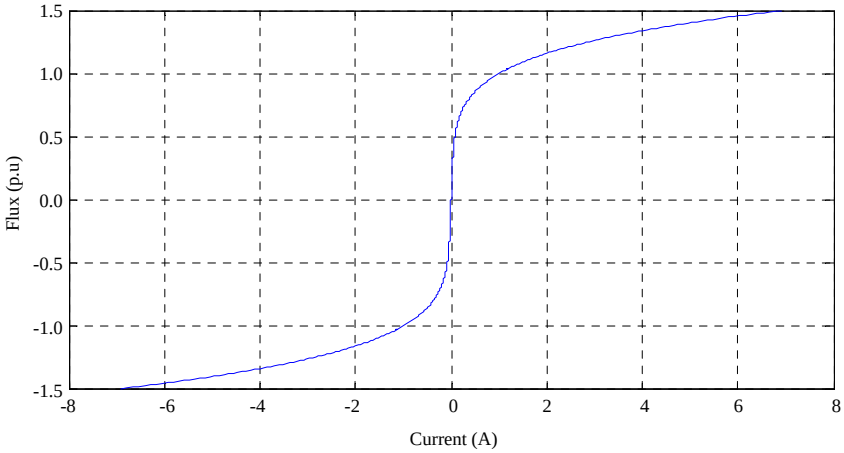

Fig. 14: Transformer magnetizing curve

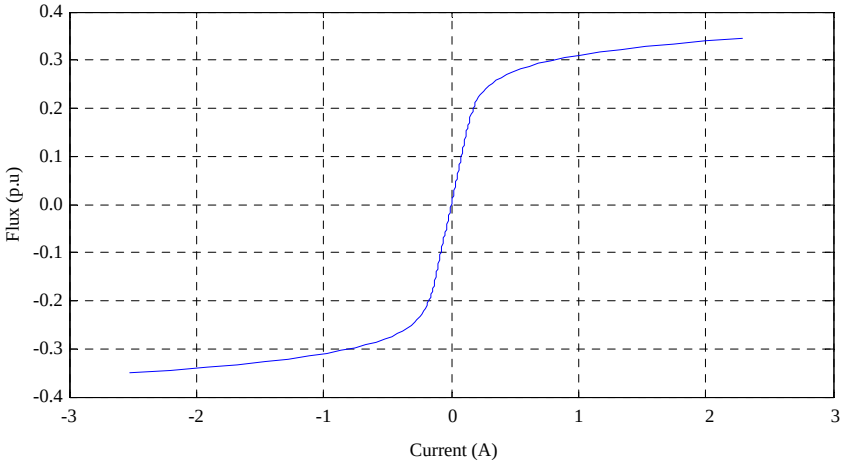

Fig. 15: Choke magnetizing curve

The saturable choke was designed with a 50 Hz knee point voltage sufficiently high to permit emergency full load operation yet low enough to provide effective damping. The saturating choke could be modelled by Eq. 35. Details of the modelled saturating choke results are shown in Fig. 15:

$$i_c(\lambda_c) = 0.8\lambda_c + .28421\lambda_c^9 \quad (35)$$

The circuit was modelled to determine the optimum damping resistor value to eliminate the unwanted ferroresonant states. Modelling showed that if the ohmic value was too high or too low the ferroresonant states would be modified but not eliminated. A damping resistor value of 6.28 Ω was selected.

Insertion of the damping resistor and saturable choke was completely effective in eliminating the ferroresonant states. The 3rd subhannonic ferroresonant state and the 2nd ferroresonant state both have been eliminated. The original 3rd subhannonic ferroresonant and the 2nd ferroresonant states can be clearly seen in the results of the uncompensated circuit.

The choke and damping resistor prevented the establishment of ferroresonance following every switching transient attempt to excite the circuit into a ferroresonant state.

The modelling results have shown how the saturable choke can eliminate the steady state 3rd subhannonic and 2nd subhannonic ferroresonant modes. The effectiveness of the saturable choke can be demonstrated by examining switch on transients that would normally lead to ferroresonance.

When energising transformers, a zero voltage switch on angle is the most severe starting condition with respect to transformer saturation and inrush currents. For a series

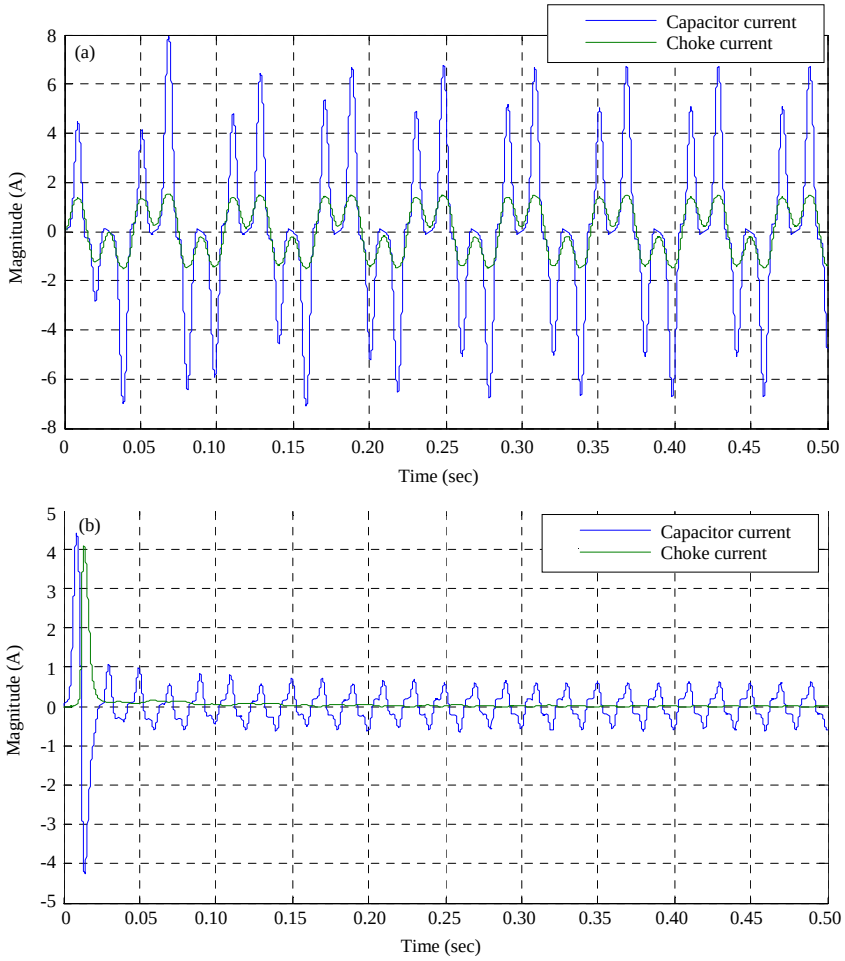

Fig. 16(a-b): Response of current and flux of (a) Circuit "B" without FL and (b) Circuit "B" with FL

compensated circuit at rest (i.e., no stored energy), a switch on at voltage zero is the condition most likely to initiate ferroresonance because of the transformer saturation and inrush current effects.

Figure 16a shows the simulated response to a zero voltage switch on without the saturable choke in place. The figure shows that after a brief transient of approximately five cycles, a stable 3rd subhannonic ferroresonance is established and continues indefinitely.

Figure 16b shows the simulation of the same series compensated circuit with the saturable choke and damping resistor added. The saturable choke and damping resistor have the effect of damping out the switch on transient in a way that does not permit the establishment of steady state ferroresonance. At 0.012s, choke current peak reaches at 4.1 pu and then returns permanently to near zero per unit after two cycles. It is the ability of the choke to provide a D.C. current path that makes the scheme so effective. Comparison of the two switch on transients show clearly the effectiveness of the saturable choke and damping resistor in eliminating ferroresonance.

Of course the impact of FL in circuit does not limited current and almost it can improve all characteristics. Figure 17-20 show simulation results for a sinusoidal voltage source 1.4 pu for circuit B with and without FL that are confirmer effect of FL on state variables and characteristics of the circuit.

According to the Fig. 17a and b can be seen when there is not FL in circuit, voltage peak of capacitor is approximately 0.9 pu and with the arrival of the FL, voltage peak of capacitor is reduced to 0.04 pu that furthur elimination of ferroresonance, reduces heat and stress in the capacitor dielectric and increases its longevity.

As in Fig. 18a and b is observed, after a short transient, FL causes remove of ferroresonance and regular loops is formed. With the elimination of the transient state from Fig.18b and 19 is obtained.

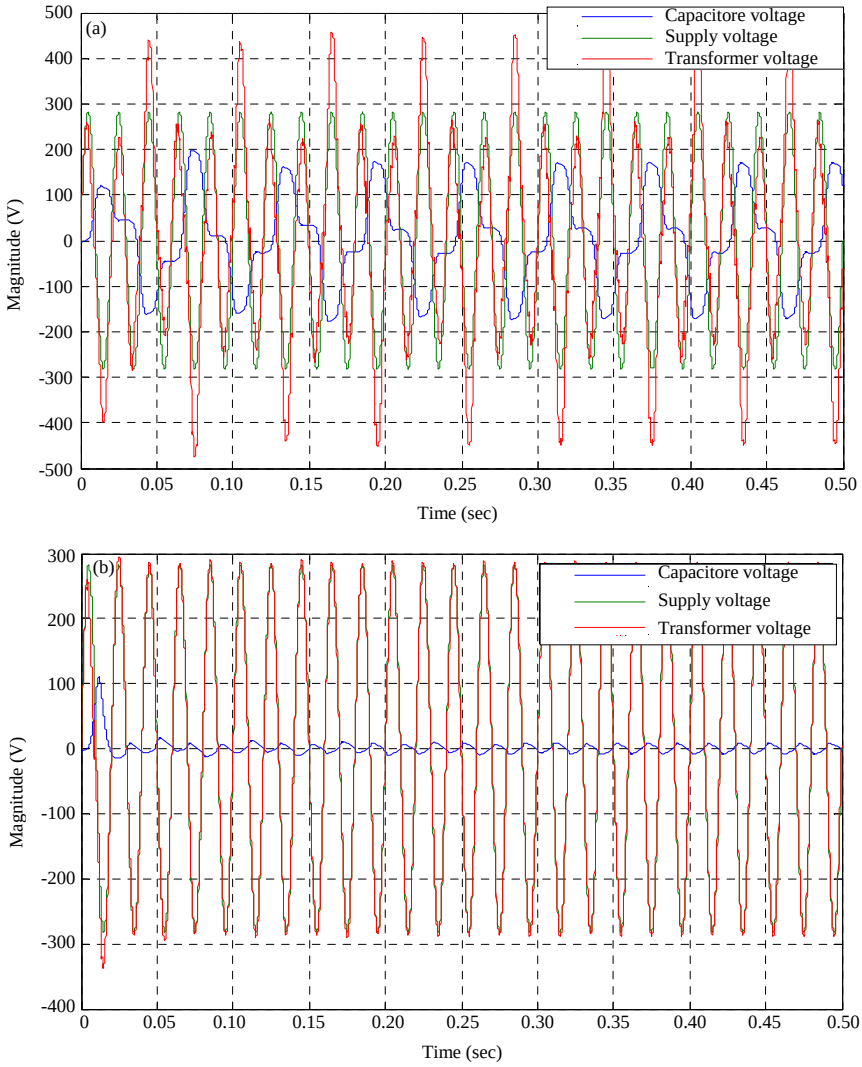

Fig. 17(a-b): Response of capacitor and transformer voltage of (a) Circuit "B" without FL and (b) Circuit "B" with FL

Also Fig. 20a, b show state plane trajectories of circuit considerate time in simulation result that is useful for understanding of performance of FL.

Selection of component values: On first inspection the selection of component values appears to be difficult requiring extensive modelling of each individual situation. Modelling and analysis of a number of circuit configurations has shown that selection of component values can be relatively straightforward by the use of the following rules.

Capacitor μF selection: To achieve full compensation the capacitor value "C" should be selected to give the same reactive impedance as the line inductance at the power frequency, i.e., for full compensation:

$$C = \frac{1}{L\omega^2} \quad (36)$$

where, ω is frequency of voltage source, L is inductance.

There are stability advantages in designing for less than full compensation. Depending on the actual design situation, engineers may elect to less than fully compensate for the inductive reactance of the line.

Damping resistor ohmic selection: Modelling and simulation has shown that the damping resistor ohmic value is critical to the effective performance of the system. If the ohmic value is too high then little current flows through the choke/resistor resulting in ineffective damping under ferroresonant and fault conditions. If the ohmic value is too low heavy currents flow

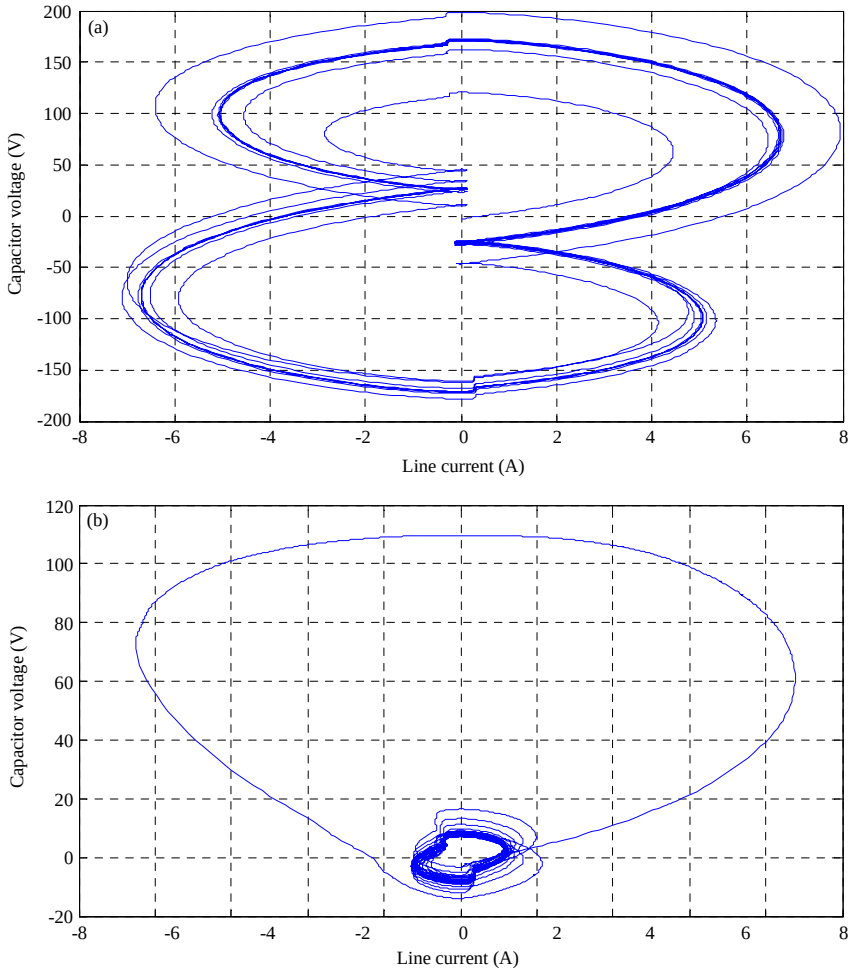

Fig. 18(a-b): State plane trajectories of (a) Circuit "B" without FL and (b) Circuit "B" with FL

through the damping resistor under ferroresonant and fault conditions but the I^2R loss is too small to provide effective damping.

Analysis and modeling on the series compensation scheme has shown damping resistor ohmic value should be selected to approximately equal the reactive impedance of the capacitor at the power frequency, i.e., suggested:

$$R_d = \frac{1}{C\omega} \quad (37)$$

where, R_d is damper resistor.

The reason for this selection is as follows. Circuit damping is provided by saturating the choke and generating I^2R losses in the damping resistor. Under conditions of choke saturation the choke can be thought of as a short circuit. Under these conditions the capacitor discharges directly into the resistor with a time constant of R_dC. At the suggested value of R_d this time constant is $1/\omega$ or $1/2\pi$ of a period. Under conditions of ferroresonance in the power line circuits the time period of high capacitor voltage is typically half to one period or 3.5-7 R_dC time constants. This is generally sufficient time for the damping resistor to sufficiently discharge the capacitor and prevent the onset of ferroresonance.

If R_d is too large the Capacitor damping resistor time constant is too long to allow effective damping. If R_d is too small the leakage reactance of the saturating choke becomes significant limiting the circulating current and hence the I^2R effect of the damping resistor. After selection of a damping resistor value R_d it is important to model and simulate the series compensation scheme to check that all ferroresonant states have been eliminated.

Saturable choke: The knee point of the saturable choke must be sufficiently high to permit normal and emergency loads without any saturation effects. However for currents in excess of the emergency load plus a safety margin the choke must go heavily into saturation.

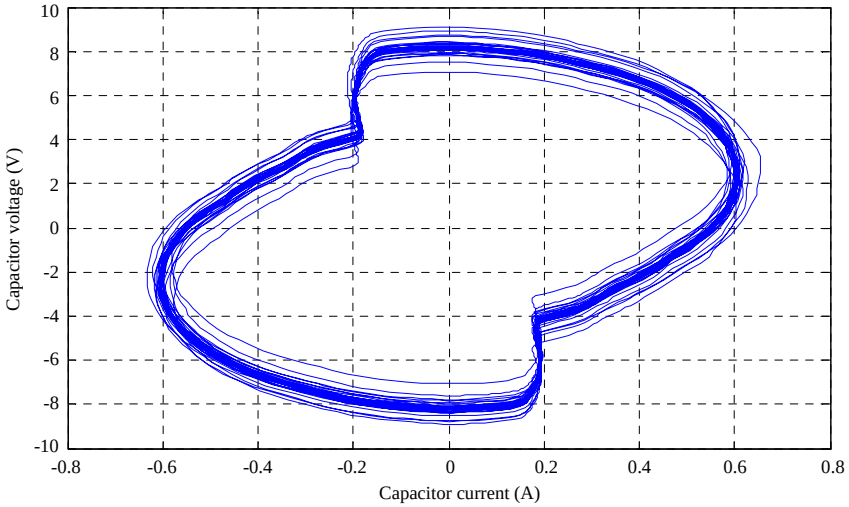

Fig. 19: State plane trajectories of circuit "B" with FL and elimination of the transient state

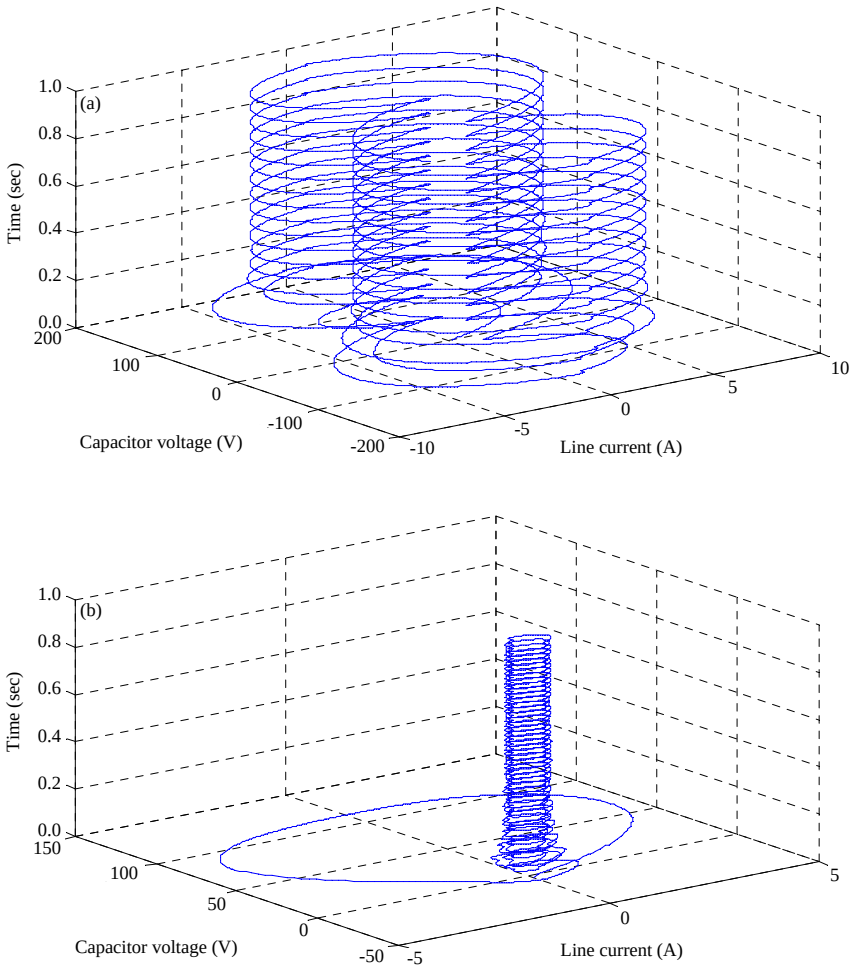

Fig. 20(a-b): State plane trajectories of (a) Circuit "B" without FL considerate time for 1s simulation and (b) Circuit "B" with FL considerate time for 1s simulation

The leakage inductance is the marginal inductance of the choke when it is in full saturation. The leakage inductance must be sufficiently small so as not to interfere with the discharge of the capacitor into the damping resistor. The ideal value would be zero henries.

To achieve the desired effect the natural frequency of the capacitor in combination with the leakage reactance of the choke (l_{cl}) must be much greater than the power frequency, i.e. suggested:

$$\frac{1}{\sqrt{l_{c1}c}} \succ\succ \omega \Rightarrow l_{c1} \prec\prec \frac{1}{c\omega^2} \quad (38)$$

In the current study a chaotic fluctuation damper device was used to reduce the ferroresonace of the power transformer. The presence of a damping resistor along with a fault current limiter reactor results in stable behavior and the removal of 2nd and 3rd order harmonics with high amplitude due to ferroresonance oscillations. In this method, the reactor eliminates the high amplitude of the energy generated in the transformer saturation range, while at the same time, the resistor with the removal of these unwanted nonlinear harmonics creates a stable behavior in the system. Using this method, it is faster than research before it uses chaos control to remove oscillations[25,28]. Also, the nonlinear order and complexity of the system will be less than recent research and in this case, the overall system analysis will be easier[11,19,21].

CONCLUSION

In this study, overvoltage and overcurrent due to ferroresonance investigated. Chaos theory is used to analyze this phenomenon. The modelling presented has highlighted the damaging ferroresonant overvoltages and overcurrents that can be created by series capacitors interacting with transformers. A thoroughly understanding of the possible ferroresonant modes of behaviour is essential when considering series compensation of distribution and subtransmission lines. A method of eliminating ferroresonance in series compensated lines has been proposed, the modelling presented has highlighted how ferroresonant overvoltages and overcurrents can be eliminated by the use of a saturable choke and damping resistor. As was observed, FL could have remove ferroresonant oscillations and causes mitigation in subharmonic regions.

SIGNIFICANCE STATEMENTS

This study is useful in analyzing and controlling the chaotic ferroresonance behavior created in the power system, which is caused by compensations by the presence of series capacitors or the effect of high transmission lines in equipment such as transformers. Chaotic harmonic over voltages are identified by using chaotic analysis tools and are limited and as far as possible eliminated by restricting the fault current limiter, reactors and damper resistances. Using this study, a better analysis of the system stability limits will be available in presence of reactive power control resources.

REFERENCES

1. Emin, Z. and Y.K. Tong, 2001. Ferroresonance experience in UK: Simulations and measurements. Proceedings of the International Conference on Power System Transients, June 24-28, 2001, Rio de Janeiro, Brazil, pp: 1-7.
2. Mukerjee, R.N., B. Tanggawelu, A.E. Ariffin and M. Balakrishnan, 2003. Indices for ferroresonance performance assessment in power distribution network. Proceedings of the International Conference on Power Systems Transients, September 28-October 2, 2003, New Orleans, Louisiana, USA., pp: 1-8.
3. Abbasi, A., M. Rostami, H. Radmanesh and H.R. Abbasi, 2009. Evaluation of chaotic ferroresonance in power transformers including nonlinear core losses. Proceedings of the IEEE Conference of EEEIC, November 2009, Wroclaw, Poland, pp: 1-7.
4. Tokic, A. and J. Smajic, 2015. Modeling and simulations of ferroresonance by using BDF/NDF numerical methods. IEEE Trans. Power Deliv., 30: 342-350.
5. Jacobson, D.A.N., 2003. Examples of ferroresonance in a high voltage power system. Proceedings of the IEEE Power Engineering Society General Meeting, July 13-17, 2003, Ontario, Canada, pp: 1206-1212.
6. Lesieutre, B.C., J.A. Mohamed and A.M. Stankovic, 2000. Analysis of ferroresonance in three-phase transformers. Proceedings of the International Conference on Power System Technology, December 4-7, 2000, Perth, WA., Australia, pp: 1013-1018.
7. Tokic, A., V. Madzarevic and I. Uglesic, 2005. Numerical calculations of three phase transformer transients. IEEE Trans. Power Deliv., 20: 2493-2500.
8. Milicevic, K., I. Flegar and D. Pelin, 2009. Flux reflection model of the ferroresonant circuit. Math. Problems Eng., Vol. 2009. 10.1155/2009/693081.

9. Laohacharoensombat, K., K. Tuitemwong, S. Jaruwattanadilok, C. Wattanasakpubal and K. Kleebmek, 2004. Case study of ferroresonance in 33 kV distribution network of PEA Thailand. Proceedings of the IEEE Region 10 Conference on TENCON, November 22-24, 2004, Chiang Mai, Thailand, pp: 417-420.
10. Sutherland, P.E. and R. Manning, 2006. Ferroresonance in a 13.8 kV distribution line. Proceedings of the 41st IAS Annual Meeting Conference Record of the IEEE Industry Applications Conference, October 8-12, 2006, Tampa, FL., USA., pp: 2238-2241.
11. Tsao, T.P. and C.C. Ning, 2006. Analysis of ferroresonant overvoltages at Maanshan nuclear power station in Taiwan. IEEE Trans. Power Deliv., 21: 1006-1012.
12. Simha, V. and W.J. Lee, 2008. The jump phenomena. IEEE Ind. Applic. Magaz., 14: 53-59.
13. Corea-Araujo, J.A., F. Gonzalez-Molina, J.A. Martinez, J.A. Barrado-Rodrigo and L. Guasch-Pesquer, 2014. Tools for characterization and assessment of ferroresonance using 3-D bifurcation diagrams. IEEE Trans. Power Deliv., 29: 2543-2551.
14. Milicevic, K., I. Rutnik and I. Lukacevic, 2008. Impact of voltage source and initial conditions on the initiation of ferroresonance. WSEAS Trans. Circuits Syst., 7: 800-810.
15. Iravani, M.R., A.K.S. Chaudhary, W.J. Giesbrecht, I.E. Hassan and A.J.F. Keri *et al*., 2000. Modeling and analysis guidelines for slow transients. III. The study of ferroresonance. IEEE Trans. Power Deliv., 15: 255-265.
16. Milicevic, K., D. Vinko and D. Vulin, 2014. Experimental investigation of impact of remnant flux on the ferroresonance initiation. Int. J. Electr. Power Energy Syst., 61: 346-354.
17. Milicevic, K., D. Vinko and D. Vulin, 2014. Experimental investigation of symmetry-breaking in ferroresonant circuit. IEEE Trans. Circuits Syst. I: Regular Papers, 61: 1543-1552.
18. Rezaei-Zare, A., R. Iravani and M. Sanaye-Pasand, 2009. Impacts of transformer core hysteresis formation on stability domain of ferroresonance modes. IEEE Trans. Power Deliv., 24: 177-186.
19. Milicevic, K., D. Pelin and I. Flega, 2008. Measurement system for model verification of nonautonomous second-order nonlinear systems. Chaos Solitons Fractals, 38: 939-948.
20. Grijalva, S., 2012. Individual branch and path necessary conditions for saddle-node bifurcation voltage collapse. IEEE Trans Power Syst., 27: 12-19.
21. Li, Y., W. Shi and F. Li, 2006. Novel analytical solution to fundamental ferroresonance-part I: Power frequency excitation characteristic. IEEE Trans. Power Syst., 21: 788-793.
22. Li, Y., W. Shi and F. Li, 2006. Novel analytical solution to fundamental ferroresonance-Part II: Criterion and elimination. IEEE Trans. Power Deliv., 21: 794-800.
23. Abbasi, H.R., v Gholami, S.H. Fathi and A. Abbasi, 2012. Analysis and investigation of effect of MOA on chaotic ferroresonant oscillations in unloaded transformer. Am. J. Scient. Res., 55: 56-69.
24. Jacobson, D.A.N., P.W. Lehn and R.W. Menzies, 2002. Stability domain calculations of period-1 ferroresonance in a nonlinear resonant circuit. IEEE Trans. Power Deliv., 17: 865-871.
25. Fordoei, H.R.A., A. Gholami, S.H. Fathi and A. Abbasi, 2015. A new approach to eliminating of chaotic ferroresonant oscillations in power transformer. Int. J. Electr. Power Energy Syst., 67: 152-160.
26. Charalambous, C.A., Z. Wang, P. Jarman and J.P. Sturgess, 2014. Time-domain finite-element technique for quantifying the effect of sustained ferroresonance on power transformer core bolts. IET Electr. Power Applic., 8: 221-231.
27. Piasecki, W., M. Florkowski, M. Fulczyk, P. Mahonen and W. Nowak, 2007. Mitigating ferroresonance in voltage transformers in ungrounded MV networks. IEEE Trans. Power Deliv., 22: 2362-2369.
28. Picher, P., L. Bolduc, B. Girard and V.N. Nguyen, 2006. Mitigation of ferroresonance induced by single-phase opening of a three-phase transformer feeder. Proceedings of the Canadian Conference on Electrical and Computer Engineering, May 7-10, 2006, Ottawa, Ont., Canada, pp: 482-485.
29. Sanaye-Pasand, M., A. Rezaei-Zare, H. Mohseni, S. Farhangi and R. Iravani, 2006. Comparison of performance of various ferroresonance suppressing methods in inductive and capacitive voltage transformers. Proceedings of the IEEE Power India Conference, April 10-12, 2006, New Delhi, India.
30. Yu, Y. and H. Zhou, 2005. Study on simulation of ferroresonance elimination in 10kV power system. Proceedings of the Asia and Pacific IEEE/PES Transmission and Distribution Conference and Exhibition, August 18, 2005, Dalian, China, pp: 1-7.
31. Yunge, L., S. Wei, R. Qin and J. Yang, 2003. A systematical method for suppressing ferroresonance at neutral-grounded substations. IEEE Trans. Power Deliv., 18: 1009-1014.
32. Abbasi, A., H. Radmanesh, M. Rostami and H. Abbasi, 2009. Elimination of chaotic ferroresonance in power transformers including nonlinear core losses applying of neutral resistance. Proceedings of the IEEE Conference of EEEIC, November 2009, Wroclaw, Poland, pp: 1-8.
33. Davarpanah, M., M. Sanaye-Pasand and F.B. Ajaei, 2012. Compensation of CVT increased error and its impacts on distance relays. IEEE Trans. Power Deliv., 27: 1670-1677.
34. Deng, J. and X.P. Zhang, 2014. Robust damping control of power systems with TCSC: A multi-model BMI approach with H_2 performance. IEEE Trans. Power Syst., 29: 1512-1521.
35. Wornle, F., D.K. Harrison and C. Zhou, 2005. Analysis of a ferroresonant circuit using bifurcation theory and continuation techniques. IEEE Trans. Power Deliv., 20: 191-196.
36. Rezaei, S., 2017. Impact of plant outage on ferroresonance and maloperation of differential protection in the presence of SVC in electrical network. IET Generation Transmission Distrib., 11: 1671-1682.

37. Nayfeh, A.H., 2004. Applied Nonlinear Dynamics: Analytical, Computational and Experimental Methods. WILEY-VCH Verlag GmbH & Co. KGaA., Weinheim, USA.
38. Al-Anbarri, K., R. Ramanujam, R. Saravanaselvan and K. Kuppusamy, 2003. Effect of iron core loss nonlinearity on chaotic ferroresonance in power transformers. Electr. Power Syst. Res., 65: 1-12.
39. Yang, M., W. Sima, Q. Yang, J. Li, M. Zou and O. Duan, 2017. Non-linear characteristic quantity extraction of ferroresonance overvoltage time series. IET Generation Transmission Distrib., 11: 1427-1433.
40. Moses, P.S., M.A.S. Masoum and H.A. Toliyat, 2011. Impacts of hysteresis and magnetic couplings on the stability domain of ferroresonance in asymmetric three-phase three-leg transformers. IEEE Trans. Energy Convers., 26: 581-592.